Nat. Hazards Earth Syst. Sci. Discuss., 2, 6173–6199, 2014
www.nat-hazards-earth-syst-sci-discuss.net/2/6173/2014/
doi:10.5194/nhessd-2-6173-2014

Natural Hazards and Earth System Sciences
Discussions
Open Access

Developing an effective 2-D urban flood inundation model for city emergency management based on cellular automata

L. Liu[1,2], Y. Liu[1], X. Wang[1], D. Yu[3], K. Liu[1], H. Huang[1], and G. Hu[4]

[1]Center of Integrated Geographic Information Analysis, School of Geography and Planning, SunYat-sen University, Guangzhou, China
[2]Department of Geography, University of Cincinnati, Cincinnati, USA
[3]Centre for Hydrological and Ecosystem Science, Department of Geography, Loughborough University, Loughborough, UK
[4]School of Geography and Planning, and Guangdong Key Laboratory for Urbanization and Geo-simulation, SunYat-sen University, Guangzhou, China

Received: 8 August 2014 – Accepted: 28 August 2014 – Published: 30 September 2014

Correspondence to: L. Liu (liulin2@mail.sysu.edu.cn)

Published by Copernicus Publications on behalf of the European Geosciences Union.

Abstract

Flash floods have occurred frequently and severely in the urban areas of South China. An effective process-oriented urban flood inundation model becomes an urgent demand for urban storm water and emergency management. This study develops an effective and flexible cellular automaton (CA) model to simulate storm water runoff and the flood inundation process during extreme storm events. The process of infiltration, inlets discharge and flow dynamic can be simulated only with little pre-processing on commonly available basic urban geographic data. In this model, a set of gravitational diverging rules are implemented in a cellular automation (CA) model to govern the water flow in a 3 × 3 cell template of a raster layer. The model is calibrated by one storm event and validated by another in a small urban catchment in Guangzhou of Southern China. The depth of accumulated water at the catchment outlet is interpreted from street monitoring sensors and verified by on-site survey. A good level of agreement between the simulated process and the reality is reached for both storm events. The model reproduces the changing extent and depth of flooded areas at the catchment outlet with an accuracy of 4 cm in water depth. Comparisons with a physically-based 2-D model (FloodMap) results show that the model have the capability of simulating flow dynamics. The high computational efficiency of CA model can satisfy the demand of city emergency management. The encouraging results of the simulations demonstrate that the CA-based approach is capable of effectively representing the key processes associated with a storm event and reproducing the process of water accumulation at the catchment outlet for making process-considered city emergency management decisions.

1 Introduction

Storm water runoff simulation models are of fundamental importance for assessing urban flooding dynamics (Chen and Adams, 2007), risk assessment (Dunn et al.,

NHESSD
2, 6173–6199, 2014

2014; Mahmoudi et al., 2013; Kubal et al., 2009; Taubenboeck et al., 2011; Tsakiris, 2014) and the evaluation of runoff quantity and quality control performance (Gilbert and Clausen, 2006; He et al., 2011). In the past decades, flash floods have occurred frequently and severely due to land use and climate change (Chang et al., 2010), especially in the urban areas of South China, which caused serious damage to urban properties and brought about many challenges to urban management, such as storm water piping, non-point source contamination, massive traffic jams, and others. Therefore, a simple, efficient and process-considered urban flood inundation model becomes an urgent demand for urban storm water and emergency management. However, due to the complexity of the urban setup and infrastructure, easy-established and fast urban flood modeling has always been a challenging task (Bidur Ghimire, 2013).

Compared to lumped hydrological models, two-dimensional (2-D) hydraulic models with high spatial details based on hydraulic equations gain better accuracy and credence in simulating the spread of water onto a wide surface area that contains complex urban feature, and can provide detailed information about the flooding dynamics. However, these models require a large amount of data, which are often difficult to obtain (Chen et al., 2012; Hunter et al., 2005a; Neal et al., 2009; Schumann et al., 2011; Zhang and Pan, 2014). Indeed, some of cities do not have detailed information on their sewer system including exact pipe junction locations and depths, pipe diameters, the intricate morphology and boundary conditions of channel and sewer networks (Zhang and Pan, 2014), especially in the mixture of ancient and emergent urban areas in the context of rapid urbanization of China. Thus, establishing a physics-based model is a hard task for most urban management. In addition, urban flooding is a fast process at a time scale of tens minutes. The calculation of the differential equations in these physics-based models is complicated and requires immense amount of time. In contrast, floodplain inundation is characterized by a slow varying phenomenon which can last hours, days or even weeks (Leandro et al., 2014), thus, the physics-based hydrologic model via calculation of the differential equations

NHESSD
2, 6173–6199, 2014

is tolerable in a floodplain inundation simulation, but impractical in the urban flooding inundation modeling and emergency management at present (Versini et al., 2010).

A variety of measures have been developed for improving the model performance, including grid coarsening (Yu and Lane, 2006a), parallelization (Lamb et al., 2009; Sanders et al., 2010; Yu, 2010), adaptive grid-based methods (Hunter et al., 2005a; Wang and Liang, 2011), complexity-reduced models (Liu and Pender, 2010), simplified governing equations (Bates et al., 2010). However, the loss of information with low resolution in grid coarsening method often lead a less accurate result, thus a sub-grid treatment (Yu, 2010; Yu and Lane, 2006b) was developed to regain some information. Although unstructured mesh method can effectively reduce the computing burden among these methods and have the potential to describe surface features, the pre-processing of model setup data is complex, especially in an urban area (Chen et al., 2012). Therefore, the requirements of these methods dot not fully meet the demand of city emergency management (Zhang and Pan, 2014). Accordingly, rapid and simplified flood inundation models (RFIM) have appeared to be common and straightforward for simulating flood inundation recently, such as RFIM (Krupka et al., 2007), rapid flood spreading model (Lhomme et al., 2008), GIS based urban inundation model (Chen et al., 2009), and flood-connected domain calculation (FCDC) (Zhang et al., 2014). Although these models have the advantages of computing efficiency and robustness, they only simulate the final inundation extent and fail to provide the flow and inundation processes.

Cellular automaton (CA) provides an alternative solution by simplifying the physics-based 2-D models, with grid-based simulation frame and allowing both time varying and geo-algebraic solution of spatial dynamics (Parsons and Fonstad, 2007). Instead of solving the differential equations iteratively within the simulation domain, the CA model describes a system on the basis of the local interactions of their constituent parts through incorporating gravitational rules to represent surface flow runoff (Burks, 1970; Di Gregorio and Serra, 1999; Wolfram, 1984). Furthermore, CA is naturally implementable through parallel computing, allowing for efficient simulations. All these

NHESSD
2, 6173–6199, 2014

characters of CA models have the tacit accordance with the requirements of city storm water and emergency management.

Since the storage cell approach was proposed by Zanobertti et al. (1970) to predict floodplain inundation, many CA models have become available in recent years for simulating braided river (Parsons and Fonstad, 2007; Thomas and Nicholas, 2002), river channels (Coulthard et al., 2002), floodplain rivers (LISFLOOD-FP) (Bates and De Roo, 2000), urban environment (Fewtrell et al., 2008, 2011). These methods discretized flood plains into fine regular grids, among which the fluxes of water is calculated according to many uniform flow formulae, mostly simplified from the Saint Venant equation or Manning's equations (Bates et al., 2010). For instance, the LOSFLOOD-FP is one of the most popular models and has been tested and improved by various scholars, including comparison with other approaches (Horritt and Bates, 2001, 2002), calibration using different data (Hunter et al., 2005a), proposing the adaptive time step (Hunter et al., 2005b), and evaluating in an urban area (Fewtrell et al., 2008, 2011; Sampson et al., 2012). Although these work have been done to predict flood inundation, the data requirements in LISFLOOD-FP model setup (5.9.6 version), such as the boundary conditions, channel geometry and friction (Bates et al., 2013), are difficult to obtain particularly in an urban area. The detailed urban features that affect the storm water drainage, including buildings, roads, curbs, inlets, and so on, are not explicitly prescribed in the model.

Therefore, this study aims to: (i) develop an easy-established and flexible CA model for simulating storm water runoff in an urban settings while considering detailed urban features only with little pre-processing on commonly available basic urban geographic data; and (ii) assess the feasibility and effectiveness of the model by using in situ observed street water depth records for city storm water and emergency management. The development of the model is described in Sect. 2. The study area is a small independent catchment in the downtown of Panyu District, Guangzhou, China. Two storm and urban flood events were chosen to validate the model (Sect. 3). Results are presented in Sect. 4, followed by discussion and summary.

NHESSD
2, 6173–6199, 2014

2 Model development

2.1 Model description

According to the underlying theory (Wolfram, 1985a, b, 1986a, b) of CA models, this study develops an urban surface runoff simulation model, considering four parameters:

$$\mathrm{CA} = \langle L, N, P, T \rangle, \quad (1)$$

L is the set of regular cells used to discretize the study area, defined as $\{(x,y)|x,y \in N, 0 \le x \le l_x, 0 \le y \le l_y\}$. N is the set of natural numbers. The model employs a 2-D lattice of regular cells to maintain consistency with DEM in space and for integration with GIS software. The Von Neumann neighborhood is employed, allowing water to be distributed to any of the four cells orthogonally surrounding a central cell at each iteration. $N = \{(0,0),(0,1),(0,-1),(1,0),(-1,0)\}$ identifies the neighborhood of each cell. At a specific time, each cell can exchange flow with all the four surrounding cells, depending on the water surface elevation. In this CA model, exchange between the central cell and the diagonal cells is completed by two time steps of the Von Neumann neighborhood exchanges.

P is the finite set of CA model parameters (Table 1) that determines the transition functions and describes the cell states, which continuously change with the iteration of the CA model. For instance, water is transmitted from the central cell to its neighbors at each iteration, which results in a corresponding change of its water depth. Cell size, elevation and infiltration threshold are maintained in time and space for each pixel. T represents the transition rules that determine the flow routing from one cell to another. During each iteration, precipitation, infiltration, and discharge to storm sewer inlets are considered within each cell. The amount and timing of flow routing from one cell to its neighboring are elaborated in Sect. 2.4.

During an urban storm event, surface water flow dynamics consists of three major processes, including infiltration to pervious surface, discharge to storm sewer system and surface runoff of excess water. Evapotranspiration can be neglected due to the

NHESSD
2, 6173–6199, 2014

short duration of and atmospheric conditions during a storm event. Sections below present the individual transition functions associated with each process.

2.2 Infiltration

The process of infiltration is represented by a temporally-varying infiltration rate for each pixel, limited by an infiltration threshold beyond which soil saturation is assumed to be reached and infiltration is no longer allowed. The infiltration threshold describes the maximum amount of surface water loss to infiltration. Different urban objects have different infiltration rates and thresholds. In this study area, for the pervious land is only of 16.57 % and the short of storm event, the following simple function is used to represents the infiltration rate in the model for easier calibrating this parameter. Once the cumulative infiltration amount is equal to or greater than the infiltration threshold, no further infiltration will occur.

$$\text{infiltration}_a(t) = R_a \cdot t, \tag{2}$$

where R_a is the infiltration rate of object a and t is the CA time step.

2.3 Mass loss to storm sewer system

In contrast to a rural catchment where infiltration is the major mode of mass loss, during an urban rainstorm event, discharge to storm sewer system also needs to be considered. Inlets are typically presented along the road edges in an urban environment, through which water can discharge to urban storm sewer systems. In the CA model developed, storm sewer inlets are explicitly represented by individual pixels. Instead of infiltration, the pixel that contains an inlet has a sink term associated with the mass loss to the underlying storm sewer system. Storm sewer surcharge is not considered in the model and it is assumed that the storm sewer system fully functions during a storm event. The rate of mass loss at inlets depends on a number of factors, including the local topography, storm sewer capacity and inlet configuration.

NHESSD
2, 6173–6199, 2014

In the model developed, we represent the rate of discharge at the inlets to storm sewer system using a method proposed by Sun (Xiuhui, 1999) (Eqs. 3 and 4).

$$Q = w \cdot C\sqrt{2gh \cdot k}. \quad (3)$$

$$D = Q/S, \quad (4)$$

where Q is the inlet discharge flow ($m^3\,s^{-1}$), w is the area of inlet (m^2), C is orifice coefficient, g is gravitational acceleration, h is allowed storage of water head of an inlet, k is orifice obstruction coefficient, S is the area of a cell,

$$\text{discharge}(t) = D \cdot t, \quad (5)$$

where D is the discharge rate of an inlet, and t is the CA time step.

2.4 Surface flow routing

After considering infiltration and inlet discharge, the rest of the storm water can form surface flow, often termed as surface runoff. An empirically derived hydrological rule known as Minimization algorithm is used in the model to represent surface runoff. This empirical method was proposed by Di Gregorio and Serra (1999) in the SCIARA model to simulate lava flow. D'Ambrosio et al. (2001) employed a similar method in the SCAVATU model and specified three internal transformations and two external interactions to simulate the behavior of soil erosion by water. Avolio et al. (2003) extended this method and proposed a new solution to overcome the problem of constant velocity and lack of precision. However, the time step was not given in the original algorithm. In this paper, the Manning's equation is combined with the minimization algorithm to calculate the amount of water routed from a central cell to its orthogonal neighboring cells in the CA model, which is an improvement of the original method.

In the CA model, the distribution of water from a central cell to its neighboring cells is based on an algorithm that aims to minimize the water surface elevation difference between cells. The minimization algorithm is given below:

NHESSD
2, 6173–6199, 2014

(a) Let wel_i denotes the water surface elevation of the central cell $i = 0$ and its neighboring cells (i = 1, 2, 3, and 4). The average water surface elevation of the cells is computed by Eq. (6);

$$av_1 = \frac{(wel_0 + \sum_{i \in A} wel_i)}{m}, \quad (6)$$

where m is the total cell count of the central cell plus the neighboring cells involved in water re-distribution (6 in step (a)).

(b) Eliminate cells with $wel_i > av_1$;

(c) Calculate the average water elevation of the remaining cells using Eq. (6) and further eliminate cells where $wel_i > av_1$;

(d) Repeat step (c) until no further cells can be eliminated;

(e) Partition the outflow from the central cell such that the remaining neighboring cells have the same elevation as the central cell.

This is illustrated in Fig. 1 using a set of cells with hypothetical elevation values.

To determine the time step of a model iteration, Manning's equation is used to calculate velocity for each pixel, defined as a function of water depth (d), surface slope (S), and roughness coefficient (n) (Eq. 7).

$$\text{velocity} = \frac{d^{2/3} S^{1/2}}{n}. \quad (7)$$

Time step is calculated for each pixel as the ratio between cell size and velocity. The minimum time step among the calculated values is used as a global time step so that stability can be maintained in the simulation.

To summarize, the combination of the minimization algorithm and Manning's equation allows the water elevation, the amount and direction of water exchange, and

NHESSD
2, 6173–6199, 2014

time taken for the exchange to occur to be calculated. At each time step, the model applies the CA rules to each cell in the following order: (i) precipitation is added to cells according to the length of the time step and precipitation rate; (ii) infiltration or inlets discharge is subtracted to obtain the current water depth in the cell; (iii) the velocity of each cell is calculated according to Manning's equation, the traverse time of each cell is obtained, and the minimum transverse time is chosen as the CA iterative time step to prevent the water from crossing a pixel in less than one time step; and (iv) the movable water is distributed to its neighboring cells following the minimization algorithm.

3 Case study and data availability

The model is tested in a 0.2 km^2 urban catchment (Fig. 2), the downtown of Panyu District, Guangzhou, China. It is one of the frequent flooding spots in the downtown area and is chosen for the purpose of model quick setup and validation. The land use map of the catchment is obtained from the local government, and the primary land use types are grass land, building, road and concrete surfaces. Around 83 % of the catchment surface is impervious. There are 96 individual storm sewer inlets in the catchment. According to Eqs. (3) and (4), the drainage rate of an inlet is calculated as 4.6 mm s^{-1}. All inlets have the same dimension (rectangle of 0.21 m^2), giving an orifice coefficient of 0.6 and obstruction coefficient of 0.67. Mark et al. (2004) suggest values between 1 and 5 m as optimal grid size to capture the main urban topographic features. The CA model is established using 5 m DEM grids, whose surface elevations over buildings are universally raised by 10 m.

The model is calibrated by a storm event occurred on 19 April 2012 (Fig. 5a) and validated by another storm on 5 September 2012 (Fig. 5b). The first storm event lasted for 1.2 h and the peak rainfall intensity reached 91 mm h^{-1} (Fig. 5). Precipitation hyetograph of a 1 min interval is presented in Fig. 5. Street monitoring CCTV records are available at the outlet of the catchment for both events. Time series of water depth is estimated with uncertainties of ±3 cm based on the traffic separation metal fences and

NHESSD
2, 6173–6199, 2014

other street marks visible in the videos reasonably well. Peak depths were validated immediately after the events based on the watermarks left on the metal fences. Time series of water depth are presented in Figs. 4a and b, which recover the inundating process and provide critical data for model calibration and validation. No surcharge was observed during the flood.

4 Results

4.1 Model calibration and sensitivity analysis

Model calibration and sensitivity analysis are undertaken for the 19 April 2012 event to obtain the optimal set of parameter values for the study site. Roughness value and infiltration rate are identified as the key parameters in the CA model. Simulation results with various combinations of roughness value and infiltration rate are shown in Table 2. Given that this is an urban site, four relatively low values of Manning's n were tested (0.01, 0.02, 0.03 and 0.04) and infiltration rate is kept at the lower end of typical infiltration values (5.8 and 11.7 mm h^{-1}).

A total of 9 simulations are used in the sensitivity analysis. These can be classified into four groups. The impermeable land and roads are all concrete surface, accounting for 51.61 % of the total area. Simulations 1–4 are used to analyze the impact of the roughness of concrete surface on model predictions. Around 31.82 % of the study site is occupied by buildings. Roughness is varied in simulations 1, 5, 6, and 7 to test its impact on flow routing. Simulations 1 and 8 are used to test the impact of roughness specification for grass land on flow prediction. Moreover, two infiltration values are used for the grass land surface (11.7 and 5.8 mm h^{-1}) to test the model response to the infiltration parameter. Results of the sensitivity analysis are shown in Fig. 3.

The model's responses to various roughness values and infiltration rates are illustrated in Fig. 3. Figure 3a demonstrates how the model reacts to the Manning's n specified for the concrete surface. With the increase of Manning's n, the simulation

NHESSD
2, 6173–6199, 2014

curve becomes smoother, and the peak water depth decreases proportionately (39.55, 38.50, 37.32, and 36.17 cm). As expected, the time of peak depth occurs later into the event (11:22, 11:24, 11:27, and 11:28 p.m.), due to the slower water movement associated with higher surface roughness. The model demonstrates a similar trend in the sensitivity analysis when the roughness for the building roof is varied (Fig. 3b). However, the magnitude is slightly smaller due to the coverage of buildings. Due to the size of the grassland (17 %), the model is relatively insensitive to the variation of the roughness parameter (Fig. 3c). In terms of the infiltration rate, with the value halved, the peak water depth reached increases by 1.6 cm and the peak depth timing is 1 min late.

Remote Mean Standard Error (RMSE) is calculated by comparing the model predicted depth with the observed depth at a one-minute interval using Eq. (8).

$$\mathrm{RMSE} = \sqrt{\frac{\sum_{i=1}^{q} \left(d_i^{\mathrm{pred}} - d_i^{\mathrm{ref}}\right)^2}{q}}, \tag{8}$$

where, for each simulation, q is number of the paired values, d_i^{pred} and d_i^{ref} are the predicted and reference water depths, respectively. The optimal set of parameter with a Manning's n value of 0.04 (grass land), 0.01 (impermeable land and road), 0.02 (building) and infiltration rate of 11.7 mm h^{-1} is found to produce the least RMSE value (3.30 cm).

4.2 Model validation

The optimal set of parameters identified in the model calibration and sensitivity analysis are used to simulate the inundation processes of the two storm events (Figs. 4 and 5). Figure 4a (10:50 p.m.) shows that at the beginning of the event, shallow water appeared but was constrained to the road surface. As the storm continued, water started to inundate the lower parts of the catchment (Fig. 4b and c, 10:58–11:06 p.m.). Thereafter,

NHESSD
2, 6173–6199, 2014

water started to accumulate around the outlet and expanded to the largest areas with maximum depth in the catchment (Fig. 4d and e, 11:14–11:22 p.m.) At the end of the storm event, when the surface runoff was less than the outlet capability, the inundated water began to decline (Fig. 4f, 11:30 p.m.).

The hydrograph of the inundation processes simulated by the established CA model for both storm events are illustrated in Fig. 5. The CCTV records obtained from local government were retained only 35 and 13 min for both events, respectively. The overall patterns of water depth predicted in the two simulations agree well with the observations. For the 19 April event, the model prediction for the rising limb of the event agrees well with the observation. The model predicted peak water depth was about 5 cm higher than the observed value in the first storm on 19 April, and was near perfect matching in the second storm on 4 September. In terms of timing, the predicted maximum water depth is reached 4 min later than the observation for the first storm, and the falling limb was much slower than the observed pattern. Overall, the Pearson correlation coefficient between model prediction and observation is 0.98, with the two-tailed p value less than 0.01. Moreover, the Nash–Sutcliffe model efficiency coefficient (Nash and Sutcliffe, 1970) was calculated to assess the predictive skill of the CA model and evaluate how consistent the predicted values match the observed. The Nash–Sutcliffe efficiency (E) is calculated to be 0.88, indicting a good level of temporal agreement. For the second event (Fig. 5b), the Pearson correlation coefficient is 0.95 (p = 0.01), and the E = 0.82.

4.3 Model comparison

To test the effectiveness of this CA model, a 2-D distributed model, the FloodMap, is used to simulate the same storm event in the study catchment (Yu, 2010; Yu and Lane, 2006a, b). Three CA grids (Fig. 6a) were carefully selected to compare the inundating process simulated by both models. The three grids are located at the discharge point of this catchment (P1), on the flow routing paths along the street (P2), and on the concrete surface between buildings (P3). The overall results simulated by both models,

NHESSD
2, 6173–6199, 2014

show very good agreement (Fig. 6). Since the two models have different discharge mechanism, the simulated results in Fig. 6 do not consider the discharge of sewer network in order to eliminate its influence on the inundation process.

For point 1, the inundated water depths by CA are marginally higher than those of FloodMap before the peak depth of CA and retain relatively stable at the end of the storm dispassion. The inundated water depths at point 2 and 3 are much lower than point 1 due to their location in the catchment, while both models give consistent simulations. According to the above comparison, the CA model is capable to simulate the urban inundation process with similar performance to a common physically-based and 2-D-distributed model.

5 Summary and discussion

This study develops an easy-established and flexible CA model to simulate storm water runoff and the flood inundation process in an urban setting for city emergency management. This CA model is established primarily by using building-corrected DEM data, plus the detailed urban land use and inlet distribution along the pipe lines, while assuming that the pipe can drain all the inflow from the inlets and ignore the surcharge of pipes. In practice, there was no surcharge observed during the two flooding events and others in the study catchment. During the two storm events on 19 April and 4 September 2012, the CA model recovered both inundation processes, which are comparable to the street water depth observed by CCTV and simulated by a physically-based 2-D model (FloodMap). This indicates that the CA model is capable to give a reliable prediction to the urban storm runoff and the inundation processes, which can provide more useful information for city emergency management. Nevertheless, the simulated water depth on 19 April 2012 was in agreement with the observations in the rising limb, it fell slower than the real situation in the falling limb. This is likely related to the constant inlet discharge rate used in the CA model. Thus, a dynamic discharge rate varied with water depth could be a good choice to improve the agreement in the

NHESSD
2, 6173–6199, 2014

falling limb. The relationship between discharge rate and water depth is non-linear, and we are collecting more observations to derive a reliable curve that can be used in the future.

This CA model is tested at a grid size of 5 m in a small urban catchment for the purpose of model quick setup and validation. At such a small catchment, the computing time for simulating the 1.2 h storm event on 19 April 2012 is less than 5 min for both the CA model and FloodMap at similar environment and hard ware setting. Although it is hard to tell the computing efficiency between both models, the computational efficiency of CA model can satisfy the demand of city emergency management. In addition, DEM accuracy and grid size have a great impact on inundation simulation, especially on the catchment boundary, routing path, and inundated water volume/depth. The optimal resolution of DEM for explicit expressing topography in the CA model can be tested with various resolutions to improve the accuracy of the model. Currently, the available finest DEM grid size is 5 m, and we are implementing an airborne LIDAR data collection, which can obtain finer DEM grid size of 0.5 m with higher accuracy and in a much larger area of near 20 km^2. Thus, we can test the effects of different DEM grid size on the performance of the CA model and its computing efficiency. Furthermore, parallel computing and simulation can also be tested even for a large metropolitan area for the purpose of city storm water and emergency management.

Acknowledgements. This work was supported by National High Technology Research and Development Program of China (863 Program) (No. 2012AA121402, 2012AA121403) and National Basic Research Program of China (973 Program) (No. 2012CB955903) Foundations. An anonymous reviewer is also acknowledged.

References

Avolio, M. V., Crisci, G. M., D Ambrosio, D., Di Gregorio, S., Iovine, G., Rongo, R., and Spataro, W.: An extended notion of Cellular Automata for surface flows modelling, WSEAS Trans. Comput., 2, 1080–1085, 2003.

NHESSD
2, 6173–6199, 2014

Bates, P. D. and De Roo, A. P. J.: A simple raster-based model for flood inundation simulation, J. Hydrol., 236, 54–77, 2000.
Bates, P. D., Horritt, M. S., and Fewtrell, T. J.: A simple inertial formulation of the shallow water equations for efficient two-dimensional flood inundation modelling, J. Hydrol., 387, 33–45, 2010.
Bidur Ghimire, A. S. C. M.: Formulation of a fast 2-D urban pluvial flood model using a cellular automata approach, J. Hydroinform., 15, 676–686, 2013.
Burks, A. W.: Essays on Cellular Automata, University of Illinois Press, Paris, 1970.
Chang, L.-C., Shen, H.-Y., Wang, Y.-F., Huang, J.-Y., and Lin, Y.-T.: Clustering-based hybrid inundation model for forecasting flood inundation depths, J. Hydrol., 385, 257–268, 2010.
Chen, A. S., Evans, B., Djordjevi, S., and Savi, D. A.: Multi-layered coarse grid modelling in 2-D urban flood simulations, J. Hydrol., 470/471, 1–11, 2012.
Chen, J. and Adams, B. J.: Development of analytical models for estimation of urban stormwater runoff, J. Hydrol., 336, 458–469, 2007.
Chen, J., Hill, A. A., and Urbano, L. D.: A GIS-based model for urban flood inundation, J. Hydrol., 373, 184–192, 2009.
Coulthard, T. J., Macklin, M. G., and Kirkby, M. J.: A cellular model of Holocene upland river basin and alluvial fan evolution, Earth. Surf. Proc. Land., 27, 269–288, 2002.
D'Ambrosio, D., Di Gregorio, S., Gabriele, S., and Gaudio, R.: A Cellular Automata model for soil erosion by water, Phys. Chem. Earth (B), 26, 33–39, 2001.
Di Gregorio, S., and Serra, R.: An empirical method for modelling and simulating some complex macroscopic phenomena by cellular automata, Future Gener. Comp. Sy., 259–271, 1999.
Dunn, G., Harris, L., Cook, C., and Prystajecky, N.: A comparative analysis of current microbial water quality risk assessment and management practices in British Columbia and Ontario, Canada, Sci. Total. Environ., 468/469, 544–552, 2014.
Fewtrell, T. J., Bates, P. D., Horritt, M., and Hunter, N. M.: Evaluating the effect of scale in flood inundation modelling in urban environments, Hydrol. Process., 22, 5107–5118, 2008.
Fewtrell, T. J., Duncan, A., Sampson, C. C., Neal, J. C., and Bates, P. D.: Benchmarking urban flood models of varying complexity and scale using high resolution terrestrial LiDAR data, Phys. Chem. Earth, 36, 281–291, 2011.
Gilbert, J. K. and Clausen, J. C.: Stormwater runoff quality and quantity from asphalt, paver, and crushed stone driveways in Connecticut, Water. Res., 40, 826–832, 2006.

NHESSD
2, 6173–6199, 2014

He, J., Valeo, C., Chu, A., and Neumann, N. F.: Prediction of event-based stormwater runoff quantity and quality by ANNs developed using PMI-based input selection, J. Hydrol., 400, 10–23, 2011.
Horritt, M. S. and Bates, P. D.: Predicting floodplain inundation: raster-based modelling vs. the finite-element approach, Hydrol. Process., 15, 825–842, 2001.
Horritt, M. S. and Bates, P. D.: Evaluation of 1-D and 2-D numerical models for predicting river flood inundation, J. Hydrol., 268, 87–99, 2002.
Hunter, N. M., Bates, P. D., Horritt, M. S., De Roo, A. P. J., and Werner, M. G. F.: Utility of different data types for calibrating flood inundation models within a GLUE framework, Hydrol. Earth Syst. Sci., 9, 412–430, doi:10.5194/hess-9-412-2005, 2005a.
Hunter, N. M., Horritt, M. S., Bates, P. D., Wilson, M. D., and Werner, M. G. F.: An adaptive time step solution for raster-based storage cell modelling of floodplain inundation, Adv. Water. Resour., 28, 975–991, 2005b.
Krupka, M., Pender, G., Wallis, S., Sayers, P. B., and Mulet-Marti, J.: A rapid flood inundation model, in: Proceedings of the Congress – International Association for Hydraulic Research, 32, p. 28, 2007.
Kubal, C., Haase, D., Meyer, V., and Scheuer, S.: Integrated urban flood risk assessment – adapting a multicriteria approach to a city, Nat. Hazards Earth Syst. Sci., 9, 1881–1895, doi:10.5194/nhess-9-1881-2009, 2009.
Lamb, R., Crossley, M., and Waller, S.: A fast two-dimensional floodplain inundation model, Proc. Ice-Water Manage., 162, 363–370, 2009.
Leandro, J., Chen, A. S., and Schumann, A.: A 2-D parallel diffusive wave model for floodplain inundation with variable time step (P-DWave), J. Hydrol., 517, 250–259, 2014.
Lhomme, J., Sayers, P. B., Gouldby, B. P., Samuels, P. G., Wills, M., and Mulet-Marti, J.: Recent development and application of a rapid flood spreading method, in: FLOODrisk 2008, 30 September–2 October 2008, Keble College, Oxford, UK, 2008.
Liu, Y. and Pender, G.: A new rapid flood inundation model, in: Proceedings of the first IAHR European Congress, Edinburgh, 4–6, 2010.
Mahmoudi, H., Renn, O., Vanclay, F., Hoffmann, V., and Karami, E.: A framework for combining social impact assessment and risk assessment, Envirom. Impact. Asses., 43, 1–8, 2013.
Mark, O., Weesakul, S., Apirumanekul, C., Aroonnet, S. B., and Djordjevi, S.: Potential and limitations of 1-D modelling of urban flooding, J. Hydrol., 299, 284–299, 2004.

NHESSD
2, 6173–6199, 2014

Nash, J. and Sutcliffe, J.: River flow forecasting through conceptual models part I — a discussion of principles, J. Hydrol., 10, 282—290, 1970.
Neal, J. C., Bates, P. D., Fewtrell, T. J., Hunter, N. M., Wilson, M. D., and Horritt, M. S.: Distributed whole city water level measurements from the Carlisle 2005 urban flood event and comparison with hydraulic model simulations, J. Hydrol., 368, 42–55, 2009.
Parsons, J. A. and Fonstad, M. A.: cellular automata model of surface water, Hydrol. Process., 2189–2195, 2007.
Sampson, C. C., Fewtrell, T. J., Duncan, A., Shaad, K., Horritt, M. S., and Bates, P. D.: Use of terrestrial laser scanning data to drive decimetric resolution urban inundation models, Adv. Water. Resour., 41, 1–17, 2012.
Sanders, B. F., Schubert, J. E., and Detwiler, R. L.: ParBreZo: a parallel, unstructured grid, Godunov-type, shallow-water code for high-resolution flood inundation modeling at the regional scale, Adv. Water. Resour., 33, 1456–1467, 2010.
Schumann, G. J. P., Neal, J. C., Mason, D. C., and Bates, P. D.: The accuracy of sequential aerial photography and SAR data for observing urban flood dynamics, a case study of the UK summer 2007 floods, Remote. Sens. Envirom., 115, 2536–2546, 2011.
Taubenböck, H., Wurm, M., Netzband, M., Zwenzner, H., Roth, A., Rahman, A., and Dech, S.: Flood risks in urbanized areas – multi-sensoral approaches using remotely sensed data for risk assessment, Nat. Hazards Earth Syst. Sci., 11, 431–444, doi:10.5194/nhess-11-431-2011, 2011.
Thomas, R. and Nicholas, A. P.: Simulation of braided river flow using a new cellular routing scheme, Geomorphology, 43, 179–195, 2002.
Tsakiris, G.: Flood risk assessment: concepts, modelling, applications, Nat. Hazards Earth Syst. Sci., 14, 1361–1369, doi:10.5194/nhess-14-1361-2014, 2014.
Versini, P.-A., Gaume, E., and Andrieu, H.: Application of a distributed hydrological model to the design of a road inundation warning system for flash flood prone areas, Nat. Hazards Earth Syst. Sci., 10, 805–817, doi:10.5194/nhess-10-805-2010, 2010.
Wang, J. P. and Liang, Q.: Testing a new adaptive grid-based shallow flow model for different types of flood simulations, J. Flood Risk Manage., 4, 96–103, 2011.
Wolfram, S.: Computation theory of cellular automata, Commun. Math. Phys., 96, 15–57, 1984.
Wolfram, S.: Origins of randomness in physical systems, Phys. Rev. Lett., 55, 449–452, 1985a.
Wolfram, S.: Undecidability and intractability in theoretical physics, Phys. Rev. Lett., 54, 735–738, 1985b.

NHESSD
2, 6173–6199, 2014

Wolfram, S.: Random sequence generation by cellular automata, Adv. Appl. Math., 7, 123–169, 1986a.
Wolfram, S.: Cellular automaton fluids 1: Basic theory, J. Stat. Phys., 45, 471–526, 1986b.
Xiuhui, S.: Drainage Engineering (I), China Building Industry Press, Beijing, 1999.
Yu, D. and Lane, S. N.: Urban fluvial flood modelling using a two-dimensional diffusion-wave treatment, part 2: development of a sub-grid-scale treatment, Hydrol. Process., 20, 1567–1583, 2006a.
Yu, D. and Lane, S. N.: Urban fluvial flood modelling using a two-dimensional diffusion-wave treatment, part 1: mesh resolution effects, Hydrol. Process., 20, 1541–1565, 2006b.
Yu, D.: Parallelization of a two-dimensional flood inundation model based on domain decomposition, Environ. Modell. Softw., 25, 935–945, 2010.
Zanobetti, D., Lorger, H., Preissman, A., and Cunge, J. A.: Mekong delta mathematical model program construction, J. Waterways Harbors Div., 96, 181–199, 1970.
Zhang, S. and Pan, B.: An urban storm-inundation simulation method based on GIS, J. Hydrol., 517, 260–268, 2014.
Zhang, S., Wang, T., and Zhao, B.: Calculation and visualization of flood inundation based on a topographic triangle network, J. Hydrol., 509, 406–415, 2014.

NHESSD
2, 6173–6199, 2014

Table 1. Parameters of the CA model.

Parameters	Description
S	Size of the CA cell
T	CA time step
El	Elevation
Pre	Precipitation
Wd	Water depth
Ir	Infiltration rate
It	Infiltration threshold
Rc	Roughness coefficient
D	Drainage rate of inlets

NHESSD
2, 6173–6199, 2014

Table 2. Parameter combinations used in the sensitivity analysis.

	Manning's n				Infiltration ($mm\,h^{-1}$)
	Grass land (16.57 %)	Impermeable land (37.53 %)	Road (14.08 %)	Building (31.82 %)	Grass land
1	0.04	0.01	0.01	0.01	11.7
2	0.04	0.02	0.02	0.01	11.7
3	0.04	0.03	0.03	0.01	11.7
4	0.04	0.04	0.04	0.01	11.7
5	0.04	0.01	0.01	0.02	11.7
6	0.04	0.01	0.01	0.03	11.7
7	0.04	0.01	0.01	0.04	11.7
8	0.01	0.01	0.01	0.01	11.7
9	0.04	0.01	0.01	0.01	5.8

NHESSD
2, 6173–6199, 2014

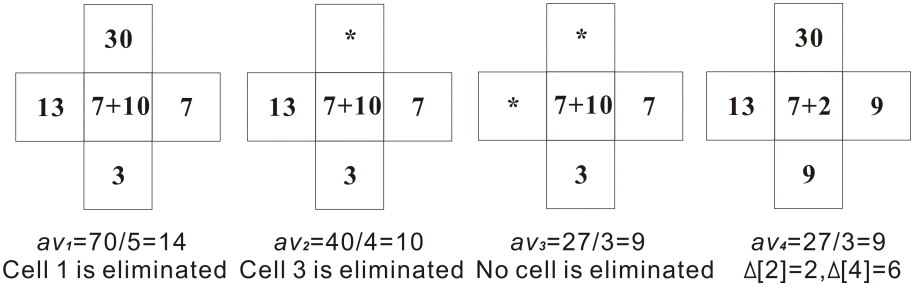

Figure 1. Example of minimization algorithm (Di Gregorio and Serra, 1999).

NHESSD
2, 6173–6199, 2014

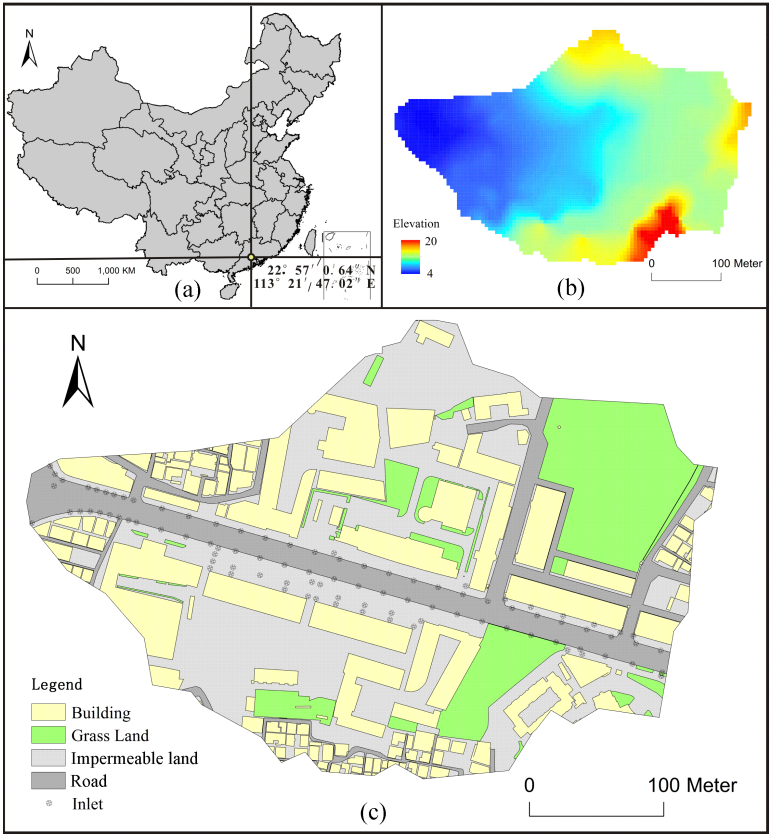

Figure 2. (a) Location of the catchment in Panyu, Guangzhou; **(b)** the surface elevation-DEM; **(c)** the components of this catchment.

NHESSD
2, 6173–6199, 2014

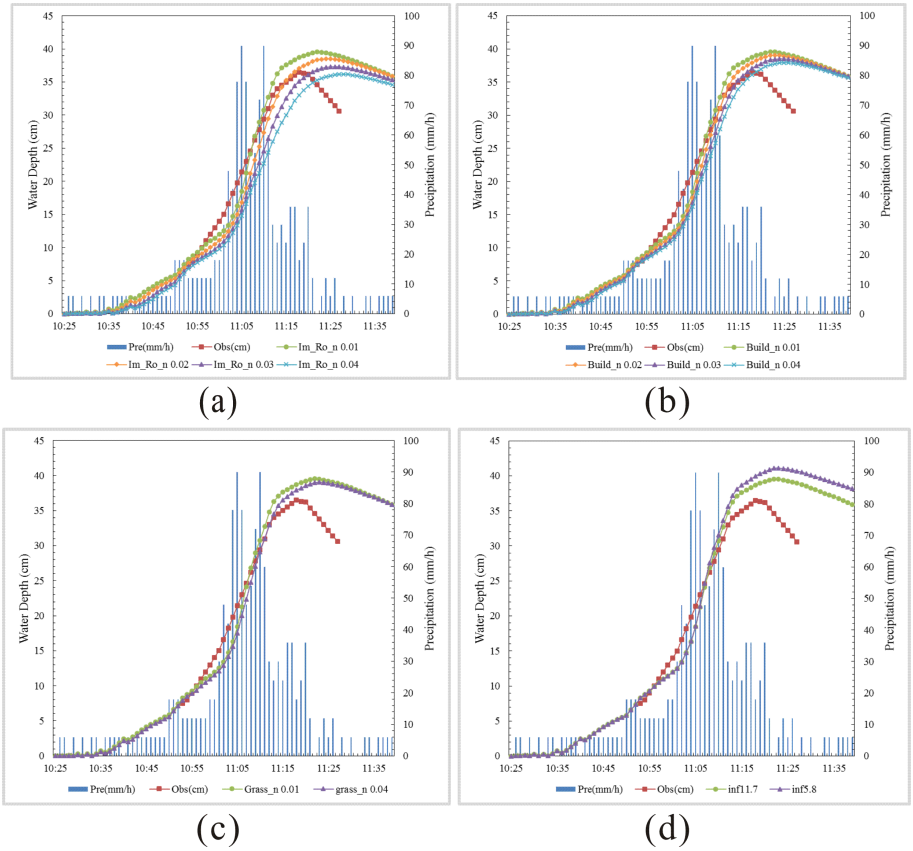

Figure 3. Results of the sensitivity analysis. **(a)** Various roughness values for the concrete surface; **(b)** various roughness values for the buildings; **(c)** various roughness values for the grassland; and **(d)** various infiltration rates for the grassland.

NHESSD
2, 6173–6199, 2014

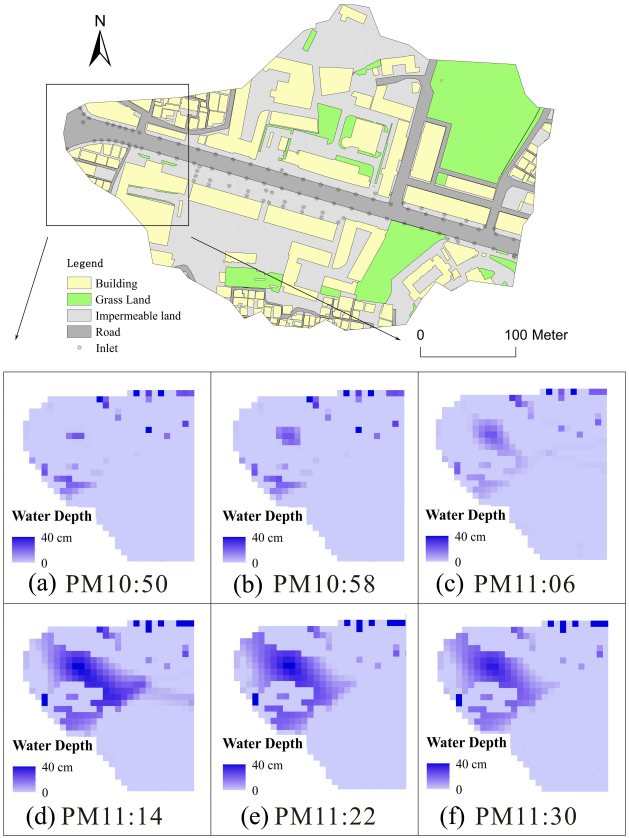

Figure 4. Process of flood inundation for the 19 April 2012 event.

NHESSD
2, 6173–6199, 2014

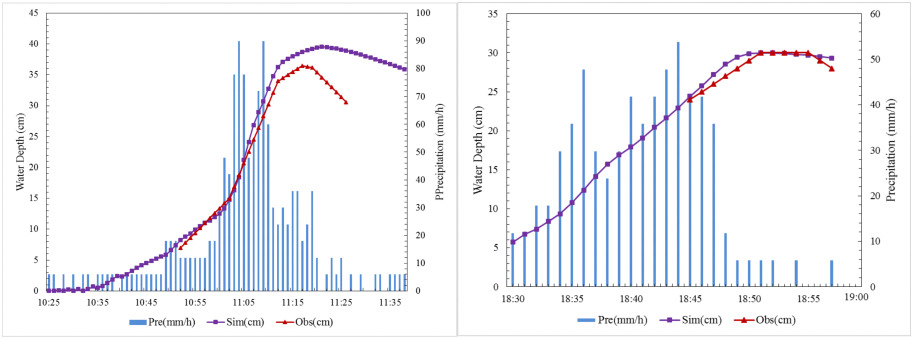

Figure 5. Time series of precipitation ($mm\,h^{-1}$) and observed water depth (cm) during the **(a)** 19 April and **(b)** 5 September 2012 events.

NHESSD
2, 6173–6199, 2014

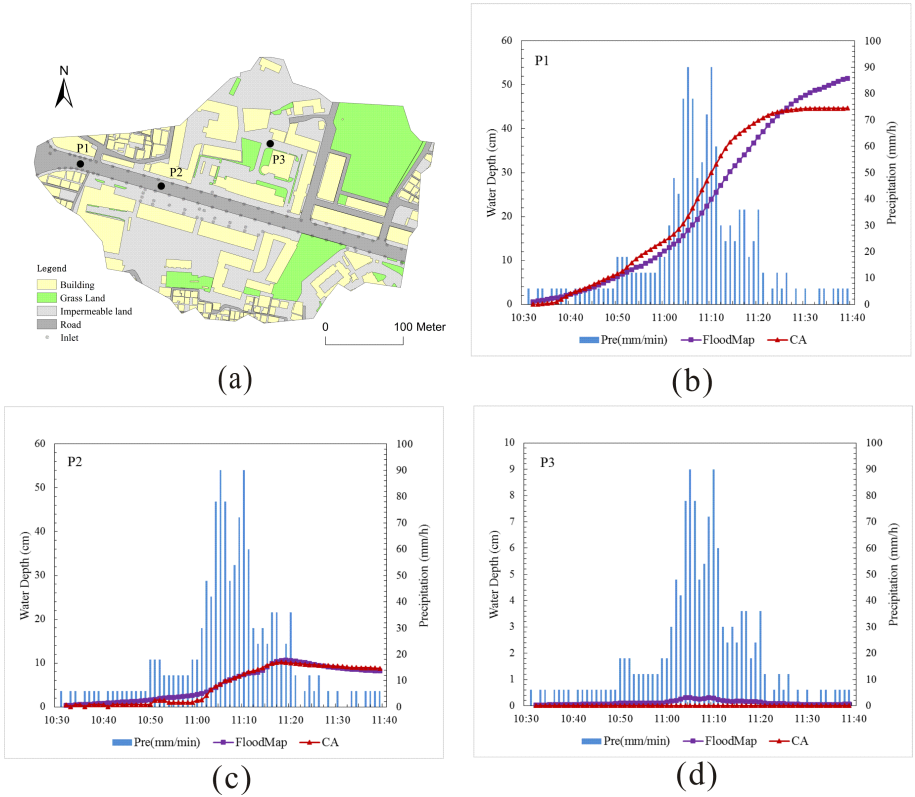

Figure 6. (a) Locations of selected grids; **(b)**, **(c)** and **(d)** temporal variation of water depth simulated by FloodMap and CA model at three selected grids.

NHESSD
2, 6173–6199, 2014